

Article

Reliability-Based and Cost-Oriented Product Optimization Integrating Fuzzy Reasoning Petri Nets, Interval Expert Evaluation and Cultural-Based DMOPSO Using Crowding Distance Sorting

Zhaoxi Hong ^{1,2}, Yixiong Feng ^{1,2,*} , Zhongkai Li ³, Guangdong Tian ^{4,*} and Jianrong Tan ^{1,2}

¹ State Key Laboratory of Fluid Power and Mechatronics Systems, Zhejiang University, Hangzhou 310027, China; hzhx@zju.edu.cn (Z.H.); egi@zju.edu.cn (J.T.)

² Key Laboratory of Advanced Manufacturing Technology of Zhejiang Province, Zhejiang University, Hangzhou 310027, China

³ School of Mechatronics Engineering, University of Mining and Technology, Xuzhou 221116, China; lizk_0202@163.com

⁴ Transportation College, Jilin University, Changchun 130020, China

* Correspondence: fyxtv@zju.edu.cn (Y.F.); tiangd2013@gmail.com (G.T.); Tel.: +86-186-6821-1935 (Y.F.); +86-137-7785-6791 (G.T.)

Received: 4 July 2017; Accepted: 31 July 2017; Published: 4 August 2017

Featured Application: By integrating fuzzy reasoning Petri Nets, interval expert evaluation and cultural-based dynamic multi-objective particle swarm optimization (DMOPSO) using crowding distance sorting, the proposed reliability-based and cost-oriented product optimization method is effective to conduct the early product design. A reasonable reliability optimization design scheme can be output, and it is of important guiding significance for the product detailed design. The superiority of the proposed method lies in its outstanding ability to deal with the uncertainties information and dynamic product failure propagation.

Abstract: In reliability-based and cost-oriented product optimization, the target product reliability is apportioned to subsystems or components to achieve the maximum reliability and minimum cost. Main challenges to conducting such optimization design lie in how to simultaneously consider subsystem division, uncertain evaluation provided by experts for essential factors, and dynamic propagation of product failure. To overcome these problems, a reliability-based and cost-oriented product optimization method integrating fuzzy reasoning Petri net (FRPN), interval expert evaluation and cultural-based dynamic multi-objective particle swarm optimization (DMOPSO) using crowding distance sorting is proposed in this paper. Subsystem division is performed based on failure decoupling, and then subsystem weights are calculated with FRPN reflecting dynamic and uncertain failure propagation, as well as interval expert evaluation considering six essential factors. A mathematical model of reliability-based and cost-oriented product optimization is established, and the cultural-based DMOPSO with crowding distance sorting is utilized to obtain the optimized design scheme. The efficiency and effectiveness of the proposed method are demonstrated by the numerical example of the optimization design for a computer numerically controlled (CNC) machine tool.

Keywords: FRPN; reliability optimization design; DMOPSO; cultural algorithm; uncertainty; interval expert evaluation

1. Introduction

Modern products are becoming more and more complex, and their reliability level has an important influence on the development of the modern manufacturing industry. Thus, it is imperative to improve the product reliability optimization design [1]. It is an important analytical tool to enhance the inherent reliability of products, and the reasonable and effective reliability optimization design has a guiding significance for the later product detailed design [2,3]. At the same time, the product cost is also a determining factor which can decide their market competitiveness, and, during application in practical engineering, the product optimal design scheme with high reliability and minimum cost is often desired by designers and customers [4,5]. The reliability-based and cost-oriented product optimization has been a hot area of research for several years [6,7]. The main common problems for the reliability optimization design of sophisticated mechatronic products are unquantifiable relationships among subsystems, modules, and components, as well as uncertain and insufficient product data. This results in the infeasibility of the methods which rely purely on mathematical algorithms. Although many efforts have been conducted on it, the efficient and effective method of reliability optimization design is still a pressing need because the conventional methods have some shortcomings that can not be ignored.

Firstly, most conventional methods fail to process the uncertain information with effect in the product optimization design [8]. Uncertainty is a commonly encountered case in the initial stage of design because of the difficulties in collecting accurate data, due to, for example, the limitations of cost, time and resource [9,10]. Therefore, reasonable reliability optimization design methodologies must have the ability to deal with such uncertainties [11,12]. Bayesian theory and fuzzy mathematics were the initiate instruments to handle the uncertainties in conventional reliability optimization design [13,14]. Ren et al. [15] put forward the multi-attribute group decision-making (MAGDM) with the integration of techniques for order preference by similarity to ideal solution (TOPSIS) and interval-valued intuitionistic fuzzy sets, which can consider the reliability of information. Zwirgmaier et al. [16] put forward to adopt Bayesian model to capture cognitive causal relation in reliability investigation, and it successfully provided a potential tool for assessing error distribution. However, the Bayesian theory depends on a subjective judgment which brings inaccurate product optimization design plans, and fuzzy mathematics needs to make their membership functions be known in advance which is almost impossible for designers.

To remedy these problems, the reliability optimization design with interval analysis was proposed where typical product variable configuration is represented using interval mathematical theory [17]. Interval analysis has recently been jointed with uncertainty algorithms, probability statistics, fuzzy mathematics, and grey system theory to get the reliability scheme with real rationality. However, these methods lack the consideration of the product failure which is linked closely with the reliability [18].

Critical product failures can bring heavy loss to economic value and society benefit, which means the analysis of product failure is essential for reliability optimization design [19–21]. Quantitative indicators of product failure are traditionally the failure frequency and failure severity, and some scholars dealt with the product reliability optimal design by the introduction of the qualitative analysis and quantitative calculation of failure mode effects analysis (FMEA) [22]. FMEA is used to describe product failure modes and their effects. It has been a powerful means to ensure product reliability, but it has three defects: (i) the relationship between the different product failures is neglected; (ii) FMEA fails to manage the uncertain product information; and (iii) FMEA regards product failure as a static process rather than a dynamic process, but it is obvious that the generation and propagation of product failure is a typical dynamic and uncertain behavior process. Hence, many extensions to the Petri net (PN) including places, transitions and directed arcs, such as colored PN, timed PN and prioritized PN, fuzzy PN have been successfully developed and applied in analyzing reliability of systems and conducting failure diagnosis [23–26]. Zhang and Yao [27] proposed an approach for analyzing systems reliability using fuzzy stochastic Petri nets (FSPNs) with fuzzy parameters, and their research successfully overcame the difficulties in adopting common software to detect multi-state

systems with high complexity. Wu and Wu [28] put forward an approach to reliability modeling and assessment by the extended object-oriented PN. Its consideration of probability statistics for product failure makes the application scope of the proposed PN become wider than that of the traditional ones. Wu et al. [29] introduced fuzzy reasoning PN (FRPN) into the reliability optimization design for highly sophisticated products, and the case study of a spacecraft solar array demonstrated its rationality and validity by its union with the fuzzy reasoning algorithm which allows it to consider stochastic interconnection between product components. However, researchers expanded the most critical influences on the product reliability optimization design, such as economic cost, state-of-the-art, performance time, and so on [30]. When the reliability design is treated as an optimization problem to solve, it is influenced by a variety of factors that can be converted into different forms of target functions or constraints. It is difficult to process and express the relationship between the various factors and the reliability indicators. The product models related to PN do not take the complexity of the product unit, importance degree, technical level and other factors into account when dealing with the influence of reliability optimization, and they fail to reflect the synthetic situation of product reliability optimization. Modern products consist of so many functional modules and components, but, in reality, reliability optimization design only needs to be conducted at the level of subsystems which consist of modules to save time and cost. These methods based on PN do not consider the subsystem division.

The objective of this paper is to develop an approach of reliability optimization design for modern mechanical products, which cannot only use the uncertain evaluation provided by experts for essential factors, subsystem division, but take into account the dynamic propagation of product failure. The interval expert evaluation is combined with the FRPN to build a reliability-based and cost-oriented product optimization model. Then, the cultural-based dynamic multi-objective particle swarm optimization (DMOPSO) using crowding distance sorting method is adopted to solve it so that the best compromise solution can satisfy the reliability constraint of the subsystem composition with minimum cost the on the maximum balance [31].

The remainder of this paper is organized as follows. Section 2 describes the general framework of the proposed method. Section 3 introduces the detail operators, and Section 4 illustrates a numerical case study of the reliability-based and cost-oriented optimization design for a CNC machine tool. Section 5 provides a comparison and analysis of the proposed method, and Section 6 offers the conclusion.

2. Framework of Proposed Method

As illustrated in Figure 1, the proposed method contains six major stages which give full consideration of uncertain expert evaluation for essential factors, subsystem division, as well as the dynamic and uncertain propagation of product failure.

- Stage I: Preparation of the product information and data

Relevant data and information are collected. First, the minimum value of product reliability allowable defined as R^* is determined according to market requirements. The reliability of a product obtained by optimization calculation is represented by R . Function module classification is conducted based on the different product sub-functions, and a set of target products are regarded as the samples to obtain the data of module failures.

- Stage II: Subsystem division based on module failure decoupling

Establish the adjacency matrix and accessibility matrix based on the module classification and data of module failures, and the subsystem division is carried out by the module failure decoupling. The detailed operator can be seen in Section 3.1.

- Stage III: Calculation of the subsystem weight considering the failure diagnosis based on FRPN

Subsystem failure diagnosis with FRPN is performed based on the data and information collected in Stage I. Principles and mathematical description of the FRPN model are introduced to build the accessibility matrix for FRPN so that the failure probability of each subsystem is available. Then, the subsystem weight considering the failure diagnosis based on FRPN can be obtained. The detailed operator can be seen in Section 3.2.

- Stage IV: Calculation of the subsystem weight considering development cost based on interval expert evaluation

Interval expert evaluation for subsystem considering development cost for six essential factors is conducted. The detailed operator can be seen in Section 3.3.

- Stage V: Establishment of the reliability-based and cost-oriented optimization model

Mathematical method aiming the product reliability and cost is established with two types of subsystem weights obtained in Stage III and Stage IV, which aim to achieve the maximum product reliability and minimum cost. The detailed operators can be seen in Section 3.4.

- Stage VI: achievement of the product optimized design solution with DMOPSO

Adopt DMOPSO to obtain the relative Pareto fronts and employ the fuzzy-based mechanism for the optimal VAR dispatch problem to extract the best compromise solution [32]. The detailed operators can be seen in Section 3.5.

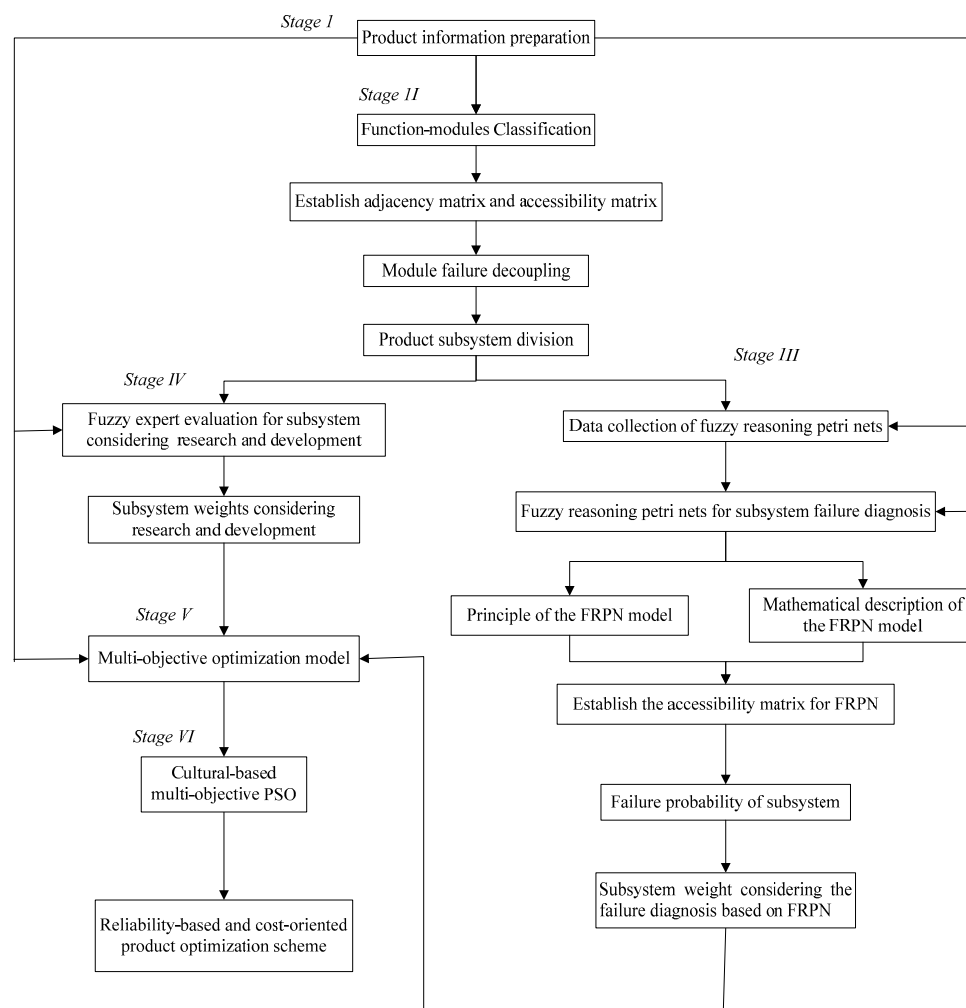


Figure 1. General framework of the proposed reliability optimization.

3. Detailed Operators

3.1. Subsystem Division Based on Failure Decoupling

This process corresponds to Stage II in Figure 1 and is described in Section 2. Reliability-based and cost-oriented product optimization deserves enough attention. In practical engineering, the product reliability optimization design only needs to be performed to the level of its subsystems because it will call for too much time and cost to apportion the product reliability to its modules and components. Hence, the reasonable subsystem division based on the function module classification is an effective guarantee for the reasonable reliability optimization. As the tight connections between product failures and reliability, the subsystem division is carried out on the module failure decoupling based on reachability matrix.

Most of the product failures can be related to certain modules, but whether the product failure is caused by the corresponding module or the connection between the corresponding module and other modules is difficult to judge. Therefore, the failure decoupling is necessary to conduct subsystem division which is used to put the function modules whose failures are related closely together to form the subsystems. We perform the classification of function modules according to the composition and working principle of products, and then conduct the data collection of module failures based on the observation of sample products. The causal relationship between modules failures is analyzed and the module failure-related mathematical model considering causal failure analysis is established.

F is the set of product module failures which consist of the collected data about module failures. a and b are the subsets of F . If the module failures in the subset b are caused by the module failures in the subset a and all the failures in subset b compose the set $A(a)$, a is the root failure sets of $A(a)$ and $A(a)$ is the relevant zone of a . Failure decoupling is the process to find the root failures according to the collected failure data whose description is:

$$\zeta = f[F; \forall x \in F, A(x); CF] \tag{1}$$

where CF is the set of product module failure in practice, and ζ is root failure sets with the calculation of function f .

The failure correlation diagram consists of a set of points $V = \{v_i\} (i = 1, 2, \dots, M)$ and a set of directed edges $E = \{e_{ij}\} (j = 1, 2, \dots, N)$. The points represent the elements of the set F . There is a directed edge from a to b if $\forall a, b \in F, b \in A(a)$. Therefore, if the failure j is caused by the failure i , there is a directed edge from i to j and there is a connection between failures i and j . These directed edges and points form the failure correlation graph. Product failure correlation graph is drawn and translated into an adjacency matrix $A = [a_{ij}]_{N \times M}$ and:

$$a_{ij} = \begin{cases} 1, & \text{if there is a directed edge form the failure } i \text{ to the failure } j (i \neq j) \text{ or } i = j \\ 0, & \text{otherwise} \end{cases} \tag{2}$$

Reachability matrix is defined to describe the extent from each connection point to another one in a directed graph via a path, which can be obtained using the time characteristics and laws of Boolean algebra. For a system consisting of n connection points which can be represented as $p_i (i = 1, 2, \dots, n)$, its reachability matrix can be denoted as $R = [a_{ij}]_{n \times m}$, and

$$a_{ij} = \begin{cases} 1, & \text{if } p_i \text{ can reach } p_j \text{ via a path } (i \neq j) \text{ or } i = j \\ 0, & \text{otherwise} \end{cases} \tag{3}$$

The reachability matrix has a significant feature which can be called as transfer characteristic. It can be described as that if the point p_i can reach the point p_k and the p_k can reach the point p_j , the point p_i can reach the point p_j . In the other words, if $a_{ik} = a_{kj} = 1$, $a_{ij} = 1$. Hence, there is a simple calculation method for the reachability matrix:

1. Build the adjacency matrix $A = (a_{ij})_{n \times n}$ based on the directed graph and its transposed matrix $A^T = (a_{ji})_{n \times n}$.
2. Analyze the y th column of the adjacency matrix A and A^T ($k = 1, 2, \dots, n$). If the element a_{xy} of A is 1 and the a_{ry} of A^T is 1, set the all the a_{xr} of A to be 1 with the adoption of permutation and combination. Establish its derivative matrix represented as M .
3. Obtain the transposed matrix of M , denoted as M^T .
4. Process the matrix M and the matrix M^T according to the above iterative criterion. Stop the iteration until the elements in M do not change as the number of iterations increases.
5. Replace all the elements in the leading diagonal of M by 1 to get the reachability matrix Φ .

The product subsystem division is obtained via module failure decoupling based on the decomposition of reachability matrix. If L_i ($i = 1, 2, \dots, k$) are the subsystems divided of the set $F = \bigcup_{i=1}^k L_i$ and $L_i \cap L_j = \emptyset(i, j)$. Based on the reachability matrix, $R(M_i)$ is the set consisting of the modules that the module M_i can reach; the set $A(M_i)$ consists of the modules which can reach the module M_i ; $C(M_i)$ is the set consisting of the common elements of $R(M_i)$ and $A(M_i)$. $B(M_i)$ is a set decided by $A(M_i)$ and $C(M_i)$. $B(M_i) = C(M_i)$ if $A(M_i) = C(M_i)$, otherwise $B(M_i) = \emptyset$. The subsystems divided can be got by the above failure decoupling, and the detailed operators can be found in Section 4.

3.2. Subsystem Weight Considering the Failure Diagnosis Based on FRPN

This process corresponds to Stage III in Figure 1, and is described in Section 2. The FRPN model considers the uncertainty of the connection between the failures of modules or subsystems in the whole product by the adoption of the fuzzy reasoning algorithm. In this section, the knowledge representation of the compound production rules based on confidence is introduced and an algorithm based on matrix operation is adopted for the formalized fuzzy reasoning. The failure diagnosis based on FRPN is good at the integration of knowledge representation with failure diagnostic reasoning so that it fits to give a dynamic description for the product failure propagation.

3.2.1. Fuzzy Production Rules

Fuzzy production rules describe the relationship between two fuzzy propositions. $E = \{e_1, e_2, \dots, e_m\}$ denotes the set of fuzzy production rules. Confidence is the degree obtained by experiences that a phenomenon could be true. The j th fuzzy production rule e_j based on the corresponding c_j is represented as: e_j (c_j): if $p_i(u_i)$, then $p_k(u_k)$, where c_j is the confidence of the fuzzy production rule e_j and it is within (0,1). p_i and p_k denote the propositions containing fuzzy variables which are difficult to describe with accurate value. u_i and u_k are the true degree of the propositions p_i and p_k , and they are also within (0,1). The truth degrees denote the fuzzy possibility of the events. A higher value indicates that the event will break down more easily. During the iteration of the truth degrees, the faults propagate in the system.

3.2.2. Definition of Fuzzy Petri Nets

The product fault tree analysis (FTA) model can be converted into the relevant FRPN model, and Wu et al. [33] described the specific conversion methods and transformation rules which are omitted in this section to make this paper more concise and compact. In brief, the AND gate in the FTA model can be regarded as many places to one transition in the FRPN model. At the same time, the OR gate in the FTA model can be regarded as many places to many transitions in FRPN model. The work in [34,35] explains in detail the particular structure of the FRPN model which is described by six elements as follows.

$P = \{p_1, p_2, \dots, p_n\}$ is the finite set of the fuzzy places, and they represent a series of fuzzy propositions;

$Trans = \{r_1, r_2, \dots, r_n\}$ is the finite set of the transitions, and they represent the implementation of fuzzy rules;

I is the directed arcs matrix from propositions to rules. $I(p_i, r_j) = 1$ if there is a directed arc from the proposition p_i to the rule r_j ; otherwise, $I(p_i, r_j) = 0$. $i = 1, 2, \dots, n; j = 1, 2, \dots, m$.

O is the directed arcs matrix from rules to propositions. $O(p_i, r_j) = 1$ if there is a directed arc from the rule r_j to the proposition p_i ; otherwise, $O(p_i, r_j) = 0$. $i = 1, 2, \dots, n; j = 1, 2, \dots, m$.

U is the true degree matrix of propositions, $u = (u_1, u_2, \dots, u_n)^T$, and u_i is within $(0, 1)$ ($i = 1, 2, \dots, n$).

$C = \text{diag} \{c_1, c_2, \dots, c_m\}$ is the confidence matrix of fuzzy production rules, and c_j is the confidence of the fuzzy production rule r_j ($j = 1, 2, \dots, n$).

3.2.3. Fuzzy Production Rules with FRPN

The input place and the output place of PN denote the precondition and conclusion of fuzzy production rules, respectively. Causal relationship between the propositions and rules is reflected by directed arcs. If the proposition is true, the token of a place is with $[0, 1]$, and the value denotes the confidence of the proposition is true. The fuzzy reasoning process is represented by the transition trigger with the confidence of fuzzy PNs.

Compared with the conventional PN, FRPN has some characteristic: (i) the token of place is within $[0, 1]$; (ii) the transition trigger denotes the true proposition happens, but the confidence of precondition remains; (iii) there is no collision which is common in the conventional PN; and (iv) there is a confidence for each transition which is within $[0, 1]$. It can be seen, that the conventional PN is a particular example of FRPN.

3.2.4. Compound Fuzzy Production Rules with FRPN

There are “and” and “or” in the precondition and conclusion of the compound fuzzy production rules, and the inexact reasoning based on confidence is adopted. Compound fuzzy production rules include four types. The related FRPNs of types 1, 2, and 3 can be seen in Figure 2a–c, respectively. The fuzzy production rule of type 4 does not guarantee a deterministic conclusion. Hence, it is not taken into consideration in FRPN.

- Type 1: $e_j(c_j) : \text{if } p_1(u_1) \text{ and } p_2(u_2) \text{ and } \dots \text{ and } p_{n-1}(u_{n-1}), \text{ then } p_n(u_n)$
 $u_n = \min(u_1, u_2, \dots, u_{n-1})c_j$
- Type 2: $e_j(c_j) : \text{if } p_1(u_1), \text{ then } p_2(u_2) \text{ and } \dots \text{ and } p_n(u_n)$
 $u_2 = u_1c_j; u_3 = u_1c_j; \dots; u_n = u_1c_j$
- Type 3: $e_j(c_j) : \text{if } p_1(u_1) \text{ or } p_2(u_2) \text{ or } \dots \text{ or } p_{n-1}(u_{n-1}), \text{ then } p_n(u_n)$
 $u_n = \max(u_1, u_2, \dots, u_{n-1})c_j$
- Type 4: $r_j(c_j) : \text{if } p_1(u_1), \text{ then } p_2(u_2) \text{ or } \dots \text{ or } p_n(u_n)$

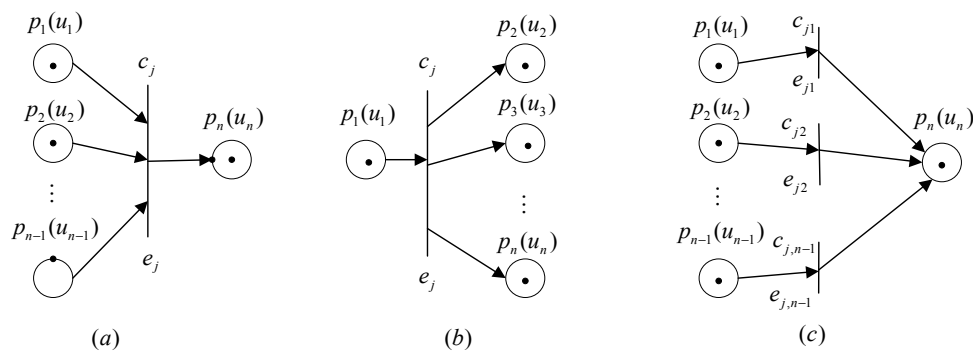


Figure 2. Compound fuzzy production rules with fuzzy PN: (a) FRPN of types 1; (b) FRPN of types 1; (c) FRPN of types 1.

3.2.5. Fuzzy Reasoning Algorithm of FRPN

Three operators are introduced to describe the fuzzy reasoning algorithm of FRPN.

Addition operator \oplus : If $g = [g_1, g_2, \dots, g_n]$ and $b = [h_1, h_2, \dots, h_n]$ are two vectors,

$$q = g \oplus h \Rightarrow q_i = \max(g_i, b_i), i = 1, 2, \dots, n. \tag{4}$$

Minimum multiplication operator \times : If G, H and Q are $m \times p, p \times n$ and $m \times n$ dimensional matrices, respectively,

$$Q_{ij} = G \times H \Rightarrow q_{ij} = \min_{1 \leq k \leq p} (g_{ik} \times h_{kj}), i = 1, 2, \dots, n. \tag{5}$$

Maximum multiplication operator \otimes : If G, H and Q are $m \times p, p \times n$ and $m \times n$ dimensional matrices, respectively,

$$q_{ij} = G \otimes H \Rightarrow q_{ij} = \max_{1 \leq k \leq p} (g_{ik} \times h_{kj}), i = 1, 2, \dots, n \tag{6}$$

Based on the definition of FRPN, the fuzzy reasoning algorithm is

$$u^{k+1} = u^k \oplus [(O \times C) \otimes (I^T \times u^k)] \tag{7}$$

The reasoning process has three steps. Firstly, $k = 0$. Secondly, obtain u^{k+1} with u^k . Thirdly, $k = k + 1$ and repeat the second step if $u^{k+1} \neq u^k$. The reasoning process is finished until $u^{k+1} = u^k$. The truth degree of the subsystem divided based on failure decoupling can be obtained. The product has n subsystems which are denoted as S_1, S_2, \dots, S_n . The truth degree of the subsystem S_i is denoted as u_i . The weight of the subsystem S_i considering product failures can be denoted as w_i^f ($i = 1, 2, \dots, n$). The subsystem weight vector considering product failures is $w_i^f = [w_1^f, w_2^f, \dots, w_n^f]$.

$$\begin{cases} w_1^f : w_2^f : \dots : w_n^f = u_1 : u_2 : \dots : u_n \\ w_1^f + w_2^f + \dots + w_n^f = 1 \end{cases} \tag{8}$$

3.3. Subsystem Weight Considering Development Cost Based on Interval Expert Evaluation

This process corresponds to Stage IV in Figure 1, and is described in Section 2. The subsystem weight considering the development cost w^1 is influenced by many factors, and its calculation is a multi-criteria decision making (MCDM) process. What should be emphasized are the difficulty and impracticality in description of the relationship between different subsystems considering different factors which have an influence on the subsystem weight considering the development cost, and there are many uncertainties unavoidable in this process. Therefore, fuzzy expert evaluation based on the interval numbers is adopted in this section. Assume the compromised variable on subsystem weight considering the development cost for i th subsystem be an interval number, $Z_i, i = 1, 2, \dots, n$ and n is the total number of subsystems. Six factors are selected to enhance the feasibility of the expert evaluation.

- Complexity (K)

Complexity can be assessed according to the number of components in a subsystem. The subsystem weight considering the development cost for a complex subsystem needs to be improved for cost saving. Thus, if a subsystem is highly complex, its weight considering the development cost tends to be high.

Hence, $Z_i \propto K_i$, where K_i is the complexity factor for the i th subsystem.

- State-of-the-art (S) factor

The novelty or technical maturity of a subsystem affects its development cost. The high technology maturity of a subsystem corresponds to low development cost.

Hence, $Z_i \propto 1/S_i$, where S_i is the state-of-the-art factor for the i th subsystem.

- Criticality of failure (C_r)

The development cost of a subsystem with critical failure effects should be improved as much as possible to prevent severe failure.

Hence, $Z_i \propto C_{ri}$, where C_{ri} is the criticality of the failure factor for the i th subsystem.

- Performance time (T)

If a subsystem is designed for a long performance time, its development cost is expected to be high to avoid frequent failures and maintenance in the process.

Hence, $Z_i \propto T_i$, where T_i is the performance time factor for the i th subsystem.

- Maintainability (M)

The maintainability of a subsystem is inversely proportional to its development cost because low reliability in a highly maintainable subsystem or components reduces product cost.

Hence, $Z_i \propto 1/M_i$, where M_i is the maintainability factor for i th subsystem.

- Environmental harshness (E)

The harshness degree of the working environment of a subsystem significantly affects subsystem development cost. The higher degree of environmental harshness of a subsystem, the higher development cost is needed to reduce frequent failures.

Hence, $Z_i \propto E_i$, where E_i is the working environment factor for the i th subsystem.

Therefore, the equation for interval values (Z_i) is expressed as follows:

$$Z_i = (K_i \times C_{ri} \times T_i \times E_i) / (M_i \times S_i) \tag{9}$$

where K_i , M_i , S_i , C_{ri} , T_i and E_i are the interval assessment values of the i th subsystem for the aforementioned factors. These variables are represented by interval numbers within [1–9] and translated into crisp numbers with the interval algorithm [36].

(x_1, y_1) and (x_2, y_2) are two interval numbers, where x_1 and x_2 , and y_1 and y_2 represent left-end and right-end points, respectively. Four fuzzy fundamental operations are shown in Equations (5)–(8), and the defuzzified value G of the interval number $G^\# = [x, y]$ is obtained by Equations (9),

$$[x_1, y_1] + [x_2, y_2] = [x_1 + x_2, y_1 + y_2] \tag{10}$$

$$[x_1, y_1] - [x_2, y_2] = [x_1 - y_2, y_1 - x_2] \tag{11}$$

$$[x_1, y_1] [x_2, y_2] = [\min(x_1 x_2, x_1 y_2, y_1 x_2, y_1 y_2), \max(x_1 x_2, x_1 y_2, y_1 x_2, y_1 y_2)] \tag{12}$$

$$[x_1, y_1] / [x_2, y_2] = [x_1, y_1] [1/y_2, 1/y_2], \text{ where } 0 \notin [x_2, y_2]s \tag{13}$$

$$G = [(x + y) + (2s - 1)(y - x)] / 2 \tag{14}$$

where s represents the caution degree of decision maker. Its value is within [0, 1] which denotes the attitude change from radicalization to caution.

The weight considering the development cost for i th subsystem w_i^d ($i = 1, 2, \dots, n$) can be available with the compromised interval number Z_i . The subsystem weight vector considering the development cost is $w_i^d = [w_1^d, w_2^d, \dots, w_n^d]$.

$$\begin{cases} w_1^d : w_2^d : \dots : w_n^d = Z_1 : Z_2 : \dots : Z_n \\ w_1^d + w_2^d + \dots + w_n^d = 1 \end{cases} \tag{15}$$

3.4. Mathematical Model of Reliability-Based and Cost-Oriented Optimization

This process corresponds to Stage V in Figure 1, and is described in Section 2. Reliability optimization is an important guarantee for the correct progression of later product detailed design. The generalized cost function is regarded as a starting point where other factors are considered. The mathematical model of reliability-based and cost-oriented product optimization is established, where the minimum product reliability allowable and the scope of subsystem reliability are regarded as constraint conditions, and the product reliability and cost are set as optimization objectives. Product cost C includes the development cost C_1 and maintenance cost C_2 .

$$C^1 = \sum_{i=1}^n C_i^1 (R_i, f_i, R_{i, \min}, R_{i, \max}, w_i^f) = \sum_{i=1}^n \exp \frac{w_i^f (1-f_i) (R_i - R_{i, \min})}{(R_{i, \max} - R_i)} \tag{16}$$

$$C^2 = \sum_{i=1}^n B_i^2 (R_i, w_i^d, C_i^2, \beta_i) = \sum_{i=1}^n B_i^2 w_i^d \exp[\beta_i (1 - R_i)] \tag{17}$$

where f_i is the feasible degree to improve the reliability of the i th subsystem; $R_{i, \min}$ is the minimum reliability of the i th subsystem after working for a while; $R_{i, \max}$ is the maximum reliability of the i th subsystem; C_i^1 is the development cost of the i th subsystem; R_i is the reliability designed of the i th subsystem which is within $[R_{i, \min}, R_{i, \max}]$; w_i^f is the weight of the i th subsystem considering the development cost; C_i^2 is the maintenance cost of the i th subsystem (all the subsystems are supposed to be repairable); B_i^2 is the purchase cost of the i th subsystem; w_i^d is the weight of the i th subsystem considering the product failure which is calculated by the FRPN model; and β_i^2 is the difficulty degree of the i th subsystem. The mathematical model of reliability-based and cost-oriented product optimization is established:

$$\begin{cases} \min C = \sum_{i=1}^n (C_i^1 + C_i^2), \\ \max R = \prod_i R_i, \\ \text{s.t. } \prod_i R_i \geq R^*, \\ R_{i, \min} \leq R_i \leq R_{i, \max} \end{cases} \quad i = 1, 2, \dots, n \tag{18}$$

where R^* is the target reliability for the product.

3.5. Adoption of Cultural-Based DMOPSO Using Crowding Distance Sorting

This process corresponds to Stage VI in Figure 1, and is described in Section 2. Compared with conventional algorithms, particle swarm optimization (PSO) is a simple and effective random algorithm to solve constrained problems [37,38]. As shown in Equation (13), the reliability-based and cost-oriented product optimization model has two optimization objectives, the maximum reliability and minimum cost, but they are negatively correlated. DMOPSO has received extensive attention by scholars in recent years [39]. The outstanding feature of DMOPSO is the combination of strong convergence ability and prominent diversity of Pareto solutions, but it still has some defects. On the one hand, the complexity of the diversity preservation for the Pareto set and global optimum update strategy brings a high computational cost. On the other hand, DMOPSO often falls into a local extreme because of its relatively scarce overall searching ability. To overcome these difficulties, cultured-based DMOPSO was proposed with the elitism strategy and crowding distance operator which brings the Pareto front closing to the accurate optimum in a more economical way [31]. Therefore, cultured-based DMOPSO using crowding distance sorting is adopted for the mathematical model of reliability-based and cost-oriented product optimization. Li et al. [31] elaborated the corresponding concrete implementing process and properties of this arithmetic.

The Pareto front has been widely used in finding the Pareto-optimal solutions to double object optimization problems. The Pareto front concept is derived from economics and engineering. It is a

straightforward way to explore the trade-offs in double objective optimization. Given a set of choices and a way of valuing them, the Pareto frontier or Pareto set is a set of choices that are Pareto efficient. The Pareto frontier is particularly useful in engineering by restricting attention to the set of choices that are Pareto-efficient. Designers can make tradeoffs within this set rather than considering the full range of every parameter.

In this paper, the Pareto front is applied to the reliability-based and cost-oriented product optimization model proposed in Section 3.4, which also has two optimization objectives: the maximum reliability and minimum cost. This product optimization model has two kinds of parameters represented by w_i^d and w_i^f ($i = 1, 2, \dots, n$, and n is the total number of subsystems of the target product obtained by the subsystem division based on failure decoupling in Section 3.1). w_i^d and w_i^f represent the weight considering the development cost of the i th subsystem and the weight considering product failures of the i th subsystem, respectively. In fact, the values of w_i^d and w_i^f in the product optimization model are computed by fuzzy logic and interval mathematics at first. Specifically, w_i^f is calculated by the fuzzy logic of FRPN in Section 3.2, and w_i^d is calculated by the interval mathematics with the method in Section 3.3. In this way, the mathematical model of reliability-based and cost-oriented optimization model proposed in this paper can be regarded as a traditional double objective optimization problem. Then, the Pareto front can be adopted to find the best solutions. In this way, the Pareto front presented in this paper is obtained with fuzzy logic. Therefore, the Pareto front in fuzzy logic is the same as the traditional Pareto front in essence.

4. Numerical Example

The computer numerically controlled (CNC) machine tools are typical modern complex products, and they are important guarantees for the sustainable development of national economy and national defense construction [40]. As a high-precision and efficient automation equipment, the failure of the CNC machine tools can cause huge loss, so it is imperative to improve the reliability of optimization design [4]. The performance of CNC machine tools has been improved drastically in recent years. At the same time, the problem of potential failures for CNC machine tools has become increasingly noticeable. Therefore, the reliability-based and cost-oriented product optimization for CNC machine tools is increasingly urgent. As shown in Figure 3, the target CNC machine tool is classified as 13 function modules according to the composition and working principle.

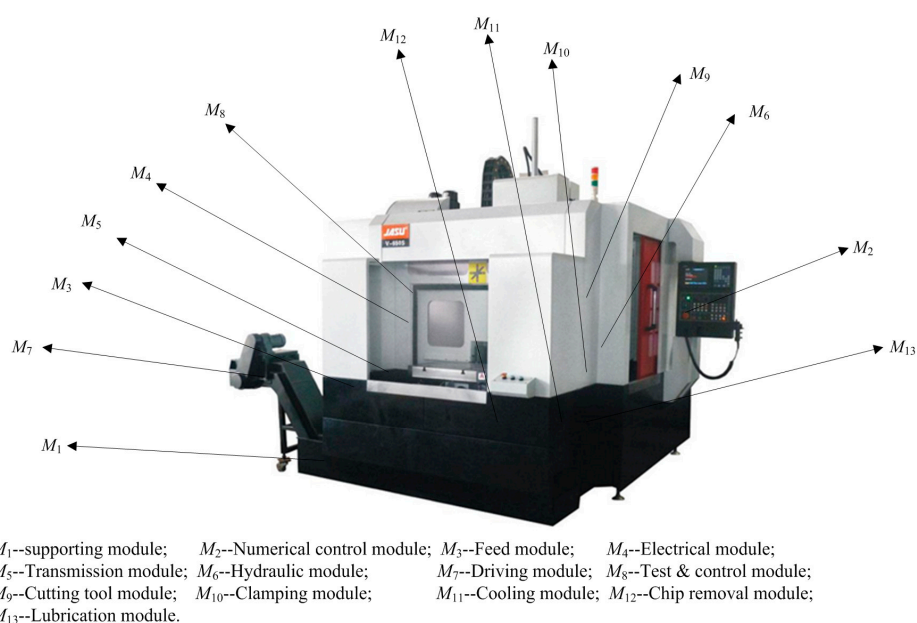


Figure 3. Function modules of the computer numerically controlled (CNC) machine tool.

4.1. Subsystem Division Based on Failure Decoupling of CNC Machine Tool

16 CNC machine tools are used to collect the module failure data, and 75 kinds of module failures are considered, as shown in Table 1. The causal relationship between modules failures is analyzed so that the failure correlation graph of the target CNC machine tool can be established, which is shown in Figure 4.

Table 1. Data about module failures for 16 computer numerically controlled (CNC) machine tools.

Number of the CNC Machine Tool	Module Failure	Number of the CNC Machine Tool	Module Failure
1	Overmuch wear of the belt Runaway speed Much noise of the hydraulic motor Noise of the main axis is abnormal The tool holder cannot rotate	9	There is a taper in the head of the machine tool Water is unable to flow into the cooling pump The lathe dose not run after programming The rotation of the main shaft is unstable Bad lubrication
2	Water leakage Loose of the protective cover Hydraulic chuck does not work The crumbs cannot be ruled out The monitor screen is not bright	10	Loss of coordinate data after power failure No input signal The knife holder cannot change the knife Bad cooling of the air-conditioning A short journey of the claw
3	Cooling water pump tripping Oil filling pipe burst The main spindle does not work No electricity can flow into the machine tool The tool holder is not located accurately	11	Z-axis stop suddenly No Lubricating oil on the guide way Low accuracy of the hydraulic chuck X-axis stop suddenly The artifact has a convex plane
4	The lathe has no input signal The tool vibrates when the workpiece is processed The noise of the main motor is abnormal The air conditioner does not work The oil pipe ruptures	12	There is motor noise when the X-axis moves The bed saddle does not move with the input of location instruction The fuse is burned out frequently X-axis Slide down after power off The servo alarm sounds the alarm
5	Automatic power off of the CNC machine tools Black lines appear on the monitor The tool will rotate automatically with the electricity The knife dish shakes The CNC machine tools do not move with the hand-cranking	13	The oil pipe ruptures The hydraulic chuck pressure cannot be raised The rotation of the main shaft is unstable The processed threads are not qualified The Stretch Speed of the stage is too slow
6	The hydraulic chuck does not work Water leakage of the machine tools The main transformer was burnt The voltage of the system drops sharply after changing the knife The speed display is not accurate	14	The machined artifacts have a taper The threading are not standard Crumbs cannot be ruled out quickly The oil pipe ruptures There is no brake when the main shaft stops turning
7	Protective glass crushing The knife cannot stop turning The finished arc is not qualified The hydraulic system cannot start A blank screen of the computer's display settings	15	The program does not run after the change of the knife A blank screen of the computer's display settings The size of the sample workpiece is inconsistent The turning operation of Z-axis is not standard The blade cannot be accurately positioned
8	X-axis can not move to the zero point Overmuch wear of the belt Cutting vibration The main shaft does not run after the system is motivated The workpiece processed have crow's feet	16	No electric current can flow into the CNC machine tools The workpiece processed have crow's feet The revolving speed of the X-axis is unstable Cutting vibration Knives cannot be replaced at will

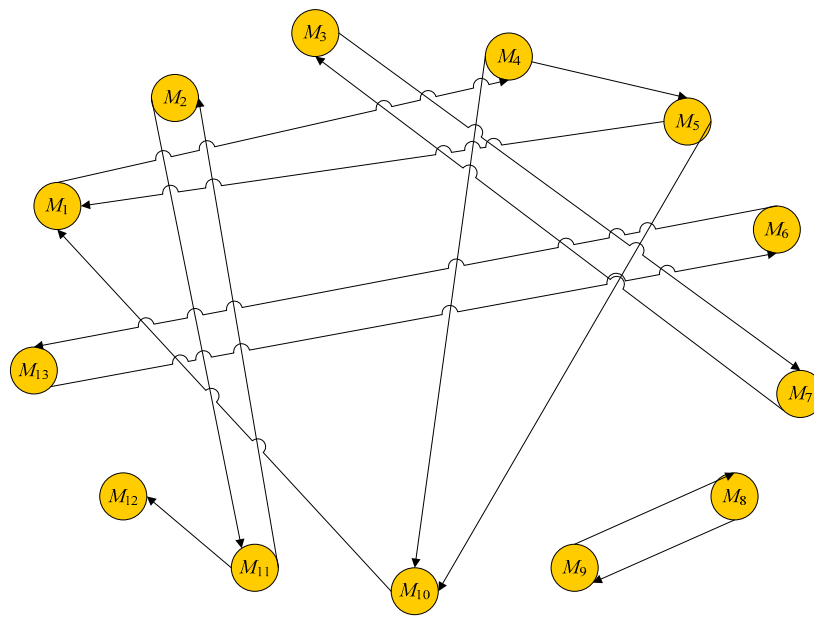


Figure 4. Failure correlation graph of the target CNC machine tool.

The failure correlation graph is drawn and translated into an adjacency matrix based on the reachability matrix that can be calculated. According to the method in Section 3.1, the subsystems of the target CNC machine tool can be divided, as shown in Figure 5.

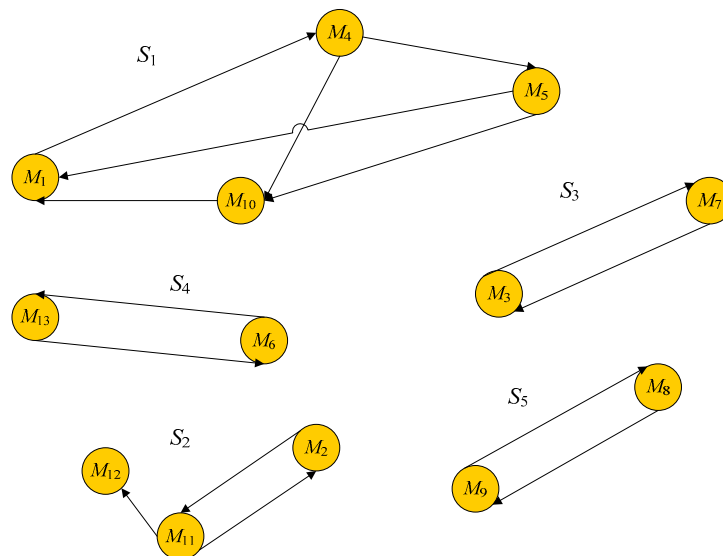


Figure 5. Subsystem division of the target CNC machine tool.

4.2. Failure Diagnosis Based on FRPN of CNC Machine Tool

Based on the main collected data about module failures in Table 1 and expert analysis, the FTA model about the CNC machine tool is available. By using the method in Section 3.2.2, which is described in detail in [33–35], the corresponding FRPN model can be converted as shown in Figure 6. In this process, the module failures listed in Table 1 that only reoccur at long intervals are removed to simplify the FRPN model of the target CNC machine tool. The relevant data about the FRPN model are collected in Tables 2 and 3 with expert evaluation and historical data analysis about the CNC machine tool.

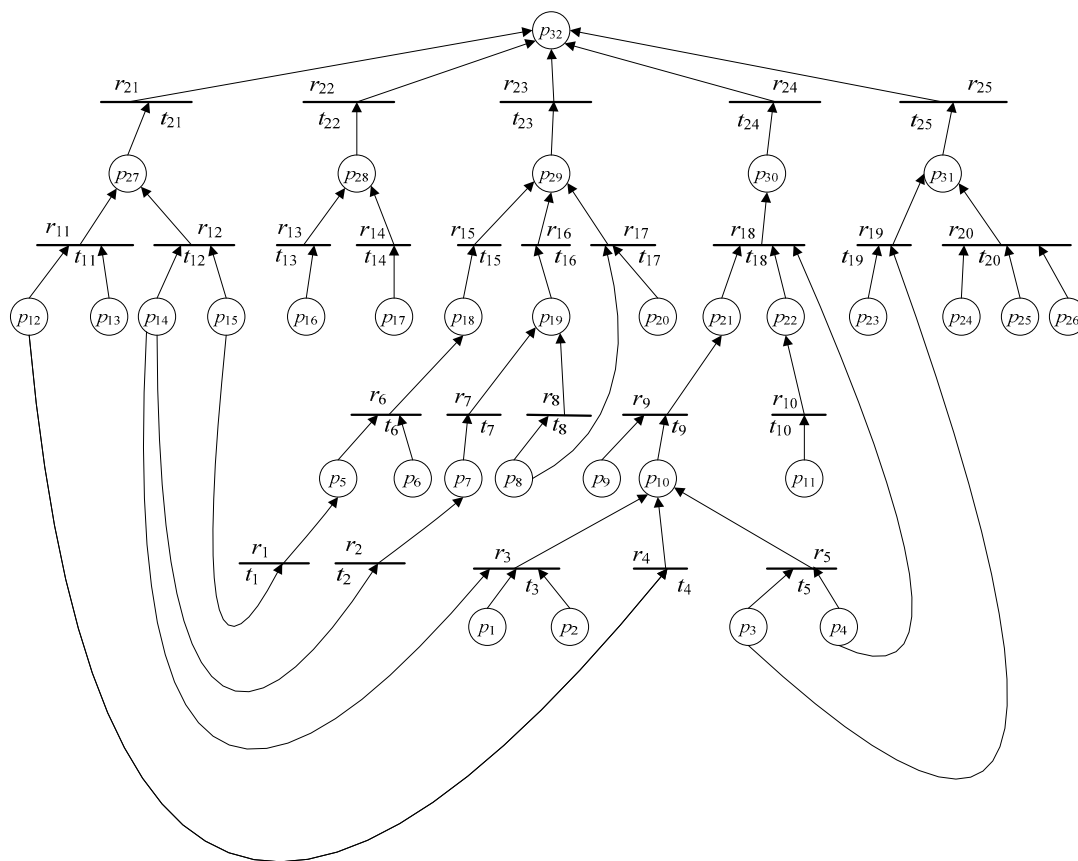


Figure 6. Fuzzy reasoning Petri Net (FRPN) model of the CNC machine tool.

Table 2. p_i and θ_i of the fuzzy reasoning Petri Net (FRPN) model for the CNC machine tool.

p_i	Failure Denoted by p_i	θ_i	p_i	Failure Denoted by p_i	θ_i
p_1	Crush of the protective cover	0.46	p_{17}	The rotation of the main shaft is unstable	0.69
p_2	Large vibration amplitude with transmission	0.51	p_{18}	The hydraulic pressure chuck sounds the alarm	-
p_3	The tool holder is not located accurately	0.62	p_{19}	The hydraulic tool holder is not flexible	-
p_4	Crumbs cannot be ruled out quickly	0.65	p_{20}	Knives cannot be replaced at will	0.90
p_5	Bad lubrication	-	p_{21}	Too much noise of the main motor	-
p_6	The external voltage is unstable	0.68	p_{22}	The sleeve does not stretch scale automatically	-
p_7	NC hardware damage	-	p_{23}	The hydraulic chuck is automatically opened when the processing is stopped	0.68
p_8	The feed speed is stable	0.82	p_{24}	There is no electric current can flow into the servo module	0.76
p_9	Lack of driving force	0.61	p_{25}	Bad cooling of the air-conditioning	0.80
p_{10}	Low detection sensitivity	-	p_{26}	The bed saddle does not move with the input of location instruction	0.55
p_{11}	Low accuracy of the closed-loop feedback	0.58	p_{27}	Failure of the S_1	-
p_{12}	Tool wear overmuch	0.70	p_{28}	Failure of the S_2	-
p_{13}	Liquid coolant leakage	0.74	p_{29}	Failure of the S_3	-
p_{14}	The pressure of the hydraulic chuck cannot be raised	0.63	p_{30}	Failure of the S_4	-
p_{15}	A blank screen of the computer's display settings	0.82	p_{31}	Failure of the S_5	-
p_{16}	X-axis can not move to the zero point	0.75	p_{32}	The CNC machine tool can not work	-

Table 3. t_j, e_j and γ_j of the FRPN for the CNC machine tool.

t_j	e_j	γ_j	t_j	e_j	γ_j
t_1	If p_{15} , then p_5	0.85	t_{14}	If p_{17} , then p_{28}	0.85
t_2	If p_{14} , then p_7	0.89	t_{15}	If p_{18} , then p_{29}	0.82
t_3	If p_{14} and p_1 and p_2 , then p_{10}	0.88	t_{16}	If p_{19} , then p_{29}	0.87
t_4	If p_{12} , then p_{10}	0.80	t_{17}	If p_8 and p_{20} , then p_{29}	0.90
t_5	If p_3 and p_4 , then p_{10}	0.90	t_{18}	If p_{21} and p_{22} and p_4 , then p_{30}	0.91
t_6	If p_5 and p_6 , then p_{18}	0.92	t_{19}	If p_{23} and p_3 , then p_{31}	0.84
t_7	If p_7 , then p_{19}	0.86	t_{20}	If p_{24} and p_{25} and p_{26} , then p_{31}	0.87
t_8	If p_8 and p_9 , then p_{19}	0.82	t_{21}	If p_{27} , then p_{32}	?
t_9	If p_{10} , then p_{21}	0.91	t_{22}	If p_{28} , then p_{32}	?
t_{10}	If p_{11} , then p_{22}	0.90	t_{23}	If p_{29} , then p_{32}	?
t_{11}	If p_{12} and p_{13} , then p_{27}	0.84	t_{24}	If p_{30} , then p_{32}	?
t_{12}	If p_{14} and p_{15} , then p_{27}	0.86	t_{25}	If p_{31} , then p_{32}	?
t_{13}	If p_{16} , then p_{28}	0.93			

Based on the methods in Section 3.2, the subsystem weight vector considering the failure diagnosis based on FRPN is obtained as $w^f = [0.165, 0.257, 0.235, 0.137, 0.206]$.

4.3. Interval Expert Evaluation for CNC Machine Tool

A team of experts are invited to give interval evaluation for the five subsystems about the six factors so that the subsystem weight considering the development cost w^1 can be calculated. The evaluation data are expressed as interval number within $[0, 9]$, as shown in Table 4.

Table 4. Interval expert evaluation for subsystems about six factors.

Subsystem/Factor	K	S	C_r	T	M	E
S_1	[2.5, 4.3]	[3.5, 5.3]	[2.1, 4.2]	[5.0, 6.8]	[6.2, 7.6]	[4.9, 7.0]
S_2	[4.3, 5.6]	[5.8, 7.7]	[4.8, 6.7]	[3.9, 5.5]	[5.6, 8.0]	[3.9, 5.8]
S_3	[6.0, 7.6]	[5.9, 7.4]	[5.3, 6.8]	[2.9, 4.5]	[4.7, 6.6]	[4.1, 5.5]
S_4	[5.9, 7.3]	[4.9, 6.6]	[3.8, 5.6]	[4.0, 5.9]	[6.3, 7.6]	[3.9, 6.2]
S_5	[5.8, 7.0]	[7.0, 8.8]	[6.2, 7.7]	[4.1, 6.2]	[4.9, 6.5]	[7.3, 8.9]

In this section, s is set to be 0.5, which means the peaceful mind of decision makers. The subsystem weight vector considering the development cost can be calculated as $w^d = [0.201, 0.260, 0.241, 0.188, 0.110]$.

4.4. Reliability-Based and Cost-Oriented Optimization and the Solution

With the calculated subsystem weights considering the failure diagnosis based on FRPN and development cost based on expert evaluation, the mathematical model of reliability-based and cost-oriented product optimization for the CNC machine tool is established. The relevant data needed are shown in Table 5.

Table 5. Relevant data needed of the multi-objective mathematical model.

S_i	f_i	$R_{i,min}$	$R_{i,max}$	β_i^2	B_i (1000 dollars)
S_1	0.7881	0.9100	0.9800	0.2781	6.4000
S_2	0.7384	0.9300	0.9950	0.1668	6.5900
S_3	0.7616	0.9300	0.9950	0.1854	8.5360
S_4	0.8085	0.9200	0.9850	0.2356	4.3300
S_5	0.8234	0.9300	0.9940	0.1541	5.6910

Culture-based DMOPSO was carried out with the Matlab software. The related operating parameters are determined as internal swarm size $popnum = 100$, external swarm size $paretymax = 100$, iteration number $maxgen = 200$, global optimum step size $cg = 2$ (cg is within $[1, 3]$), inertia weight $winertia = 0.4$, mutation probability $pmutate = 0.1$ and float mutation index $mum = 20$. The redundant particles are excluded according to the crowding distance sorting. The Pareto fronts acquired by the culture-based DMOPSO are shown in Figure 7.

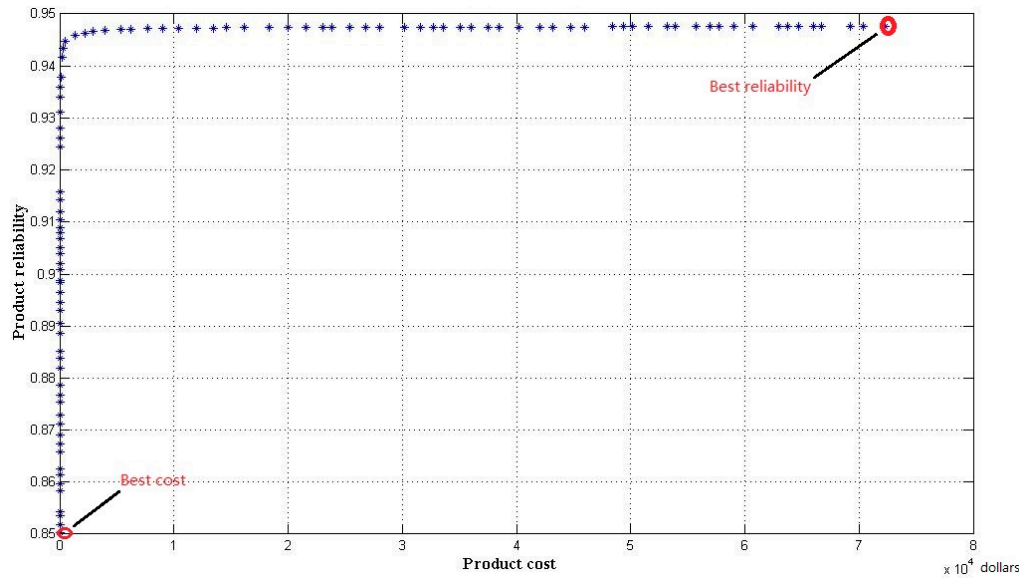


Figure 7. Complete Pareto fronts acquired by culture-based dynamic multi-objective particle swarm optimization (DMOPSO).

5. Comparison and Sensitive Analysis

5.1. Comparison

In Figure 7, it can be seen that the product cost increases slowly when the product reliability increases from 0.8500 to 0.9420, and the product cost increases sharply when the product reliability increases from 0.942 to 0.9475. The best reliability is about 0.9475 with the cost increases from 14593.1573 to 63722.7969 and the best cost is 13.1923 with the reliability equal to 0.8500. Therefore, the optimal reliability designed should within $[0.8500, 0.9420]$. For the sake of observation, part of the Pareto fronts obtained in Figure 7 is magnified, and the multi-objective algorithm for the optimal reactive power (VAR) dispatch is adopted to assess the solutions of the Pareto fronts so that the best compromise solution can be available as shown in Figure 8. Hence, the reliability-based and cost-oriented product optimization scheme for the target CNC machine tool is as follows:

$$R = 0.9090, C = 15009.2 \text{ dollars}, R_1 = 0.9705, R_2 = 0.9846, R_3 = 0.9865, R_4 = 0.9776, R_5 = 0.9863.$$

Based on Figures 7 and 8, it can be concluded that, when the product reliability and cost are selected as two optimization objectives, it is reasonable to improve moderately the product reliability from the minimum value allowed, but it is over-wasteful and meaningless to improve the product reliability to the maximum value possible. This is because the product cost is the nonlinear monotone increasing function of the product reliability, and the high cost is required to achieve high reliability. The economic cost is unlimited high to achieve the ultimate reliability which means quite a lot of money is needed to spend on the product manufacture and installation in engineering practice. In addition, the cost to improve the high product reliability is higher than that to improve the low product reliability at least to the same extent. Hence, the running results are consistent with the actual situation.

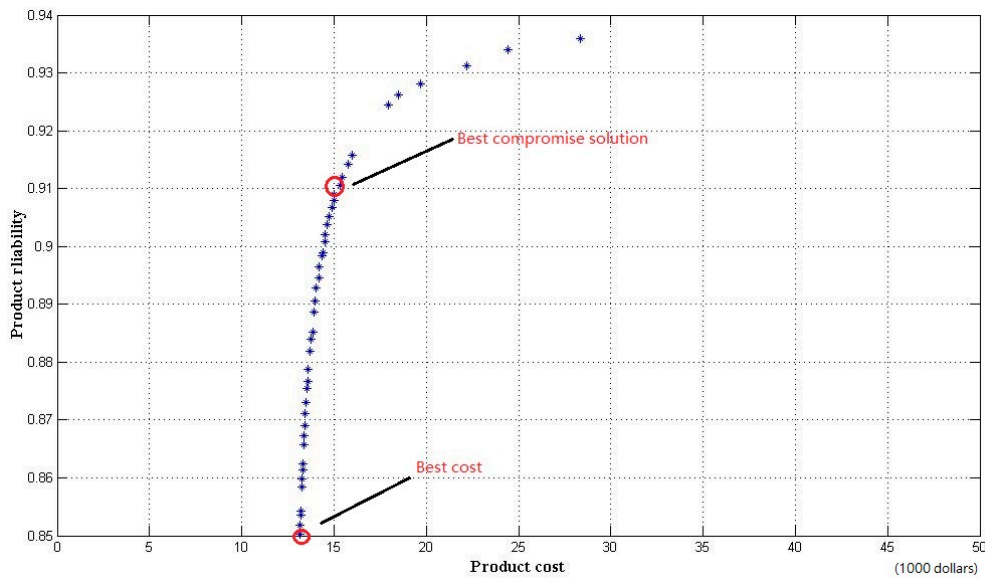


Figure 8. Best compromise solution in partial magnification of the Pareto fronts acquired by Culture-based DMOPSO.

To further discuss the best compromise solution obtained, a single objective optimization model aiming at the minimum cost is built whose corresponding constraints and parameter initialization remain the same. The results of iteration convergence are shown in Figure 9. As shown in Figure 9, the optimization design scheme is as follows:

$$R = 0.8500, C = 13139.3 \text{ dollars}, R_1 = 0.9571, R_2 = 0.9698, R_3 = 0.9733, R_4 = 0.9650, R_5 = 0.9750.$$

Therefore, the minimum cost with the reliability $R = 0.8500$ calculated with the single objective optimization model is almost the same as the best cost obtained by the proposed multi-objective mathematical model. This further validates the correctness of the proposed method.

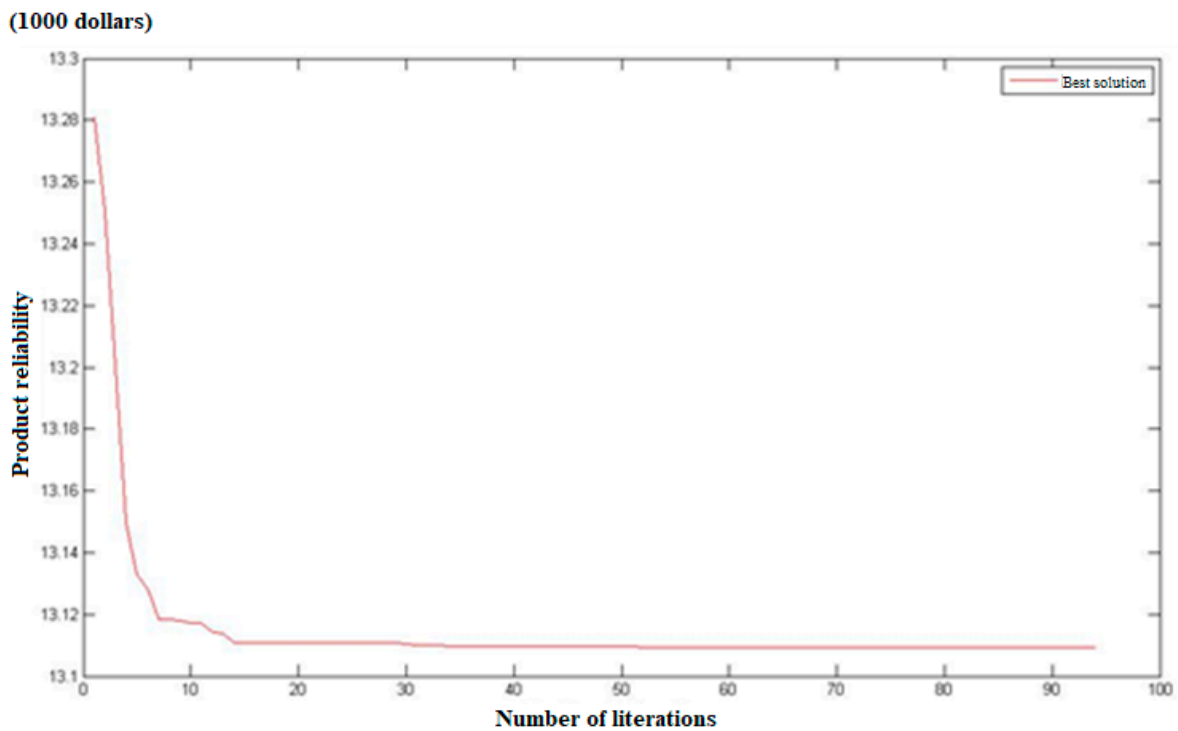


Figure 9. Pareto fronts acquired by the single objective optimization model.

5.2. Sensitivity Analysis

There is a subjective variable, the caution degree of decision maker, s , which is discovered in the implementation process of the proposed method. Hence, the sensitivity analysis is proceeded to detect the influence the subjective variable has on the results of the proposed method.

s is set to be different values to get a series of Pareto fronts which are within $[0, 1]$. The product cost tends to be prohibitive when the maximum reliability possible is achieved, and this is of no reference value for the actual product design. Therefore, it is only needed to observe the partial Pareto fronts containing the best compromise solution, which are shown in Figure 10. The related best compromise reliability optimization schemes for three different conditions are shown in Figure 11. In Figures 10 and 11, it can be seen that the partial Pareto fronts containing the best compromise solution are almost coincident as s changes, but the best compromise solution and the corresponding reliability optimization schemes are obviously different. Hence, the proposed method is sensitive to the change of s . Decision makers should put more emphasis on determining appropriate evaluation attitudes to obtain reasonable schemes.

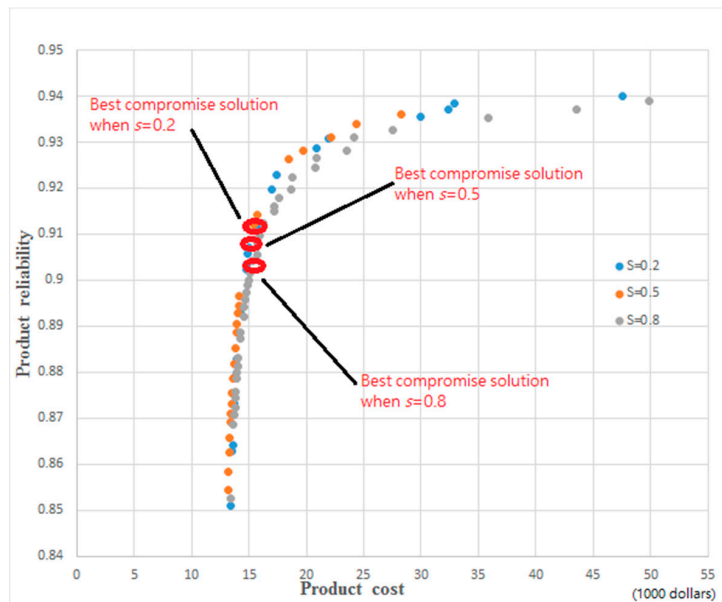


Figure 10. Partial Pareto fronts containing the best compromise solution with s .

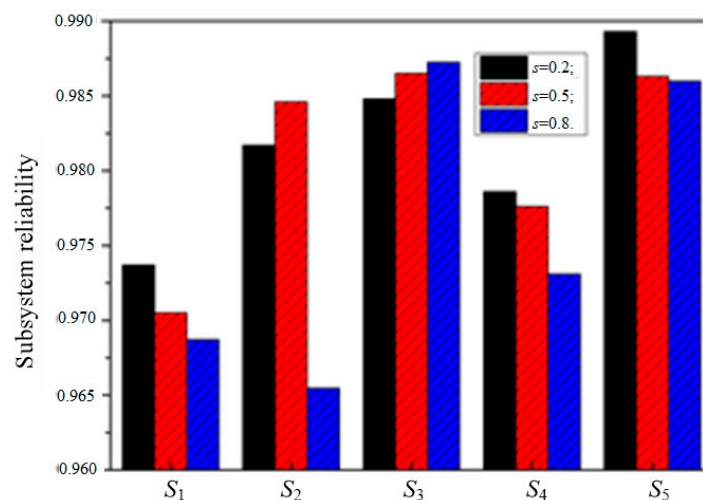


Figure 11. Best compromise reliability optimization design schemes with s .

6. Conclusions

This paper proposes a reliability-based and cost-oriented product optimization integrating FRPN, interval expert evaluation and cultural-based DMOPSO using crowding distance sorting. Based on the subsystem division with failure decoupling, it introduces FRPN to calculate the subsystem weight considering the failure diagnosis. The interval expert evaluation is adopted to calculate the subsystem weight considering development cost. Multi-objective optimization model is built with the two types of subsystem weights obtained. Cultural-based DMOPSO using crowding distance sorting is employed to get the Pareto fronts based on which the fuzzy-based mechanism picks out the best compromise solution. Compared with the conventional reliability design methods, the proposed method can not only take advantage of the uncertain expert evaluation for essential factors, but also take the dynamic and uncertain propagation of product failure into account. In addition, subsystem division with failure decoupling is performed at first so that consideration must be given to both the validity and the efficiency of the product reliability optimization design proposed. A numerical example of a CNC machine tool illustrates the practicality and efficiency of the proposed method. However, the proposed method cannot provide an effective way to consider the experts' caution degree in failure diagnosis based on FRPN, and it also fails to offer an overall analysis on how the experts' caution degree affects the best compromise solution of the product reliability design scheme. More attention should be paid to these issues in the future work of this paper. For example, a further exploration into a series of the best compromise solutions of the product reliability design with different decision maker's caution degree is indispensable to find the mathematical relationships among decision maker's caution degree, the reliability and cost obtained by the optimization calculation proposed in this paper. If the quantitative mathematical relationships can be extracted, the decision maker's caution degree can be regarded as an objective variable rather than a subjective variable. In this way, designers can invite experts with particular mentality to give their evaluation information to get the best compromise solution of the product reliability design scheme.

Acknowledgments: This work was supported by the National Natural Science Foundation of China (Grant Nos. 51490663, 51521064, and 51475459), Zhejiang Provincial Natural Science Foundation of China (No. LR14E050003), Funding for Six-Peaks Talents in Jiangsu Province (No. 2015-XXRJ-007), and Innovation Foundation of the State Key Laboratory of Fluid Power and Mechatronic Systems. Sincere appreciation is extended to the reviewers of this paper for their helpful comments.

Author Contributions: Yixiong Feng and Zhaoxi Hong conceived and designed the proposed optimal reliability design method, as well as performed the models and wrote the paper; Zhongkai Li and Guangdong Tian collected and analyzed the data; and Jianrong Tan provided the professional guidance.

Conflicts of Interest: The authors declare no conflict of interest.

References

1. Kim, H.; Kim, P. Reliability–redundancy allocation problem considering optimal redundancy strategy using parallel genetic algorithm. *Reliab. Eng. Syst. Safe.* **2017**, *159*, 153–160. [[CrossRef](#)]
2. Abouei, A.M.; Sima, M.; Zeinal, H.A.; Coit, D.W. A novel strategy for redundant components in reliability–redundancy allocation problems. *IIE Trans.* **2016**, *48*, 1043–1057. [[CrossRef](#)]
3. Conti, S.; Faraci, G.; La, C.A.; Nicolosi, R.; Rizzo, S.; Schembra, G. Effect of Islanding and Telecontrolled Switches on Distribution System Reliability Considering Load and Green-Energy Fluctuations. *Appl. Sci.* **2016**, *6*, 138. [[CrossRef](#)]
4. Zhang, Z.; Liu, Z.; Cheng, Q.; Qi, Y.; Cai, L. An approach of comprehensive error modeling and accuracy allocation for the improvement of reliability and optimization of cost of a multi-axis NC machine tool. *Int. J. Adv. Manuf. Technol.* **2016**, *89*, 561–579. [[CrossRef](#)]
5. Khorshidi, H.A.; Gunawan, I.; Ibrahim, M.Y. A value-driven approach for optimizing reliability–redundancy allocation problem in multi-state weighted k-out-of-n system. *J. Manuf. Syst.* **2016**, *40*, 54–62. [[CrossRef](#)]
6. Di, B.G.; Forcina, A.; Silvestri, A. Critical flow method: A new reliability allocation approach for a thermonuclear system. *Qual. Reliab. Eng. Int.* **2016**, *32*, 1677–1691.

7. Govindan, K.; Jafarian, A.; Azbari, M.E.; Choi, T.M. Optimal bi-objective redundancy allocation for systems reliability and risk management. *IEEE Trans. Cybern.* **2016**, *46*, 1735–1748. [[CrossRef](#)] [[PubMed](#)]
8. Chen, T.; Zheng, S.; Liao, H.; Feng, J. A multi-attribute reliability allocation method considering uncertain preferences. *Qual. Reliab. Eng. Int.* **2016**, *32*, 2233–2244. [[CrossRef](#)]
9. Cheng, J.; Tang, M.; Liu, Z.; Tan, J. Direct reliability-based design optimization of uncertain structures with interval parameters. *J. Zhejiang Univ. Sci. A* **2016**, *17*, 841–854. [[CrossRef](#)]
10. Deng, S.; Yue, D.; Fu, X.; Zhou, A. Security Risk Assessment of Cyber Physical Power System Based on Rough Set and Gene Expression Programming. *Acta Autom. Sin.* **2015**, *2*, 431–439.
11. Chang, K.H. A more general reliability allocation method using the hesitant fuzzy linguistic term set and minimal variance OWGA weights. *Appl. Soft Comput.* **2017**, *56*, 589–596. [[CrossRef](#)]
12. Chatterjee, S.; Singh, J.B.; Roy, A. A structure-based software reliability allocation using fuzzy analytic hierarchy process. *Int. J. Syst. Sci.* **2015**, *46*, 513–526. [[CrossRef](#)]
13. Tao, Y.R.; Cao, L.; Huang, Z.H.H. A novel evidence-based fuzzy reliability analysis method for structures. *Struct. Multidiscip. Optim.* **2016**, *55*, 1237–1249. [[CrossRef](#)]
14. Mishra, S.; Vanli, O.A.; Alduse, B.P.; Jung, S. Hurricane loss estimation in wood-frame buildings using Bayesian model updating: Assessing uncertainty in fragility and reliability analyses. *Eng. Struct.* **2017**, *135*, 81–94. [[CrossRef](#)]
15. Ren, H.P.; Chen, H.H.; Fei, W.; Li, D.F. A MAGDM method considering the amount and reliability information of interval-valued intuitionistic fuzzy sets. *Int. J. Fuzzy Syst.* **2016**, *19*, 715–725. [[CrossRef](#)]
16. Zwirgmaier, K.; Straub, D.; Groth, K.M. Capturing cognitive causal paths in human reliability analysis with Bayesian network models. *Reliab. Eng. Syst. Saf.* **2017**, *158*, 117–129. [[CrossRef](#)]
17. Feng, Y.; Hong, Z.; Cheng, J.; Jia, L.; Tan, J. Low carbon-oriented optimal reliability design with interval product failure analysis and grey correlation analysis. *Sustainability* **2017**, *9*, 369. [[CrossRef](#)]
18. Yang, Z.; Liu, P.; Zhu, Y.; Zhang, Y. A comprehensive reliability allocation method for series systems based on failure mode and effects analysis transformed functions. *Proc. Inst. Mech. Eng. B J. Eng. Manuf.* **2016**, *230*, 2239–2248. [[CrossRef](#)]
19. Kang, S.; Kim, E.; Shim, J.; Cho, S.; Chang, W.; Kim, J. Mining the relationship between production and customer service data for failure analysis of industrial products. *Comput. Ind. Eng.* **2017**, *106*, 137–146. [[CrossRef](#)]
20. Liu, J.; Zio, E. System dynamic reliability assessment and failure prognostics. *Reliab. Eng. Syst. Saf.* **2017**, *160*, 21–36. [[CrossRef](#)]
21. Song, L.; Fei, C.W.; Wen, J.; Bai, G.C. Multi-objective reliability-based design optimization approach of complex structure with multi-failure modes. *Aerosp. Sci. Technol.* **2017**, *64*, 52–62. [[CrossRef](#)]
22. Kim, K.O.; Yang, Y.; Zuo, M.J. A new reliability allocation weight for reducing the occurrence of severe failure effects. *Reliab. Eng. Syst. Saf.* **2013**, *117*, 81–88. [[CrossRef](#)]
23. Cheng, J.; Liu, C.; Zhou, M.C.; Zeng, Q.; Yla-Jaaski, A. Automatic Composition of Semantic Web Services Based on Fuzzy Predicate Petri Nets. *IEEE Trans. Autom. Sci. Eng.* **2015**, *12*, 680–689. [[CrossRef](#)]
24. Gao, M.M.; Zhou, M.C.; Tang, Y. Intelligent Decision Making in Disassembly Process Based on Fuzzy Reasoning Petri Nets. *IEEE Trans. Syst. Man Cybern.* **2004**, *34*, 2029–2034. [[CrossRef](#)]
25. Wang, Y.S.; Lei, H.; Han, X. The stochastic Petri net based reliability analysis for software partition integrated modular avionics. *IEEE Aerosp. Electron. Syst. Mag.* **2015**, *30*, 30–37.
26. Tang, Y.; Zhou, M.C.; Gao, M. Fuzzy-Petri-Net Based Disassembly Planning Considering Human Factors. *IEEE Trans. Syst. Man Cybern.* **2006**, *36*, 718–726. [[CrossRef](#)]
27. Zhang, X.J.; Yao, S.Z. Fuzzy stochastic Petri nets and analysis of the reliability of multi-state systems. *IET Softw.* **2015**, *9*, 83–93. [[CrossRef](#)]
28. Wu, X.; Wu, X. Mission reliability modeling and evaluation of multi-mission phased mission system based on an extended object-oriented Petri net. *Eksploracja I Niezawodnosc* **2017**, *19*, 244–253. [[CrossRef](#)]
29. Wu, J.; Yan, S.Z.; Xie, L.Y.; Gao, P. Reliability apportionment approach for spacecraft solar array using fuzzy reasoning Petri net and fuzzy comprehensive evaluation. *Acta Astronaut.* **2012**, *76*, 136–144. [[CrossRef](#)]
30. Wilson, K.J.; Quigley, J. Allocation of tasks for reliability growth using multi-attribute utility. *Eur. J. Oper. Res.* **2016**, *255*, 259–271. [[CrossRef](#)]

31. Li, Z.; Tian, G.; Cheng, G.; Liu, H.; Cheng, Z. An integrated cultural particle swarm algorithm for multi-objective reliability-based design optimization. *Proc. Inst. Mech. Eng. C J. Mech. Eng. Sci.* **2013**, *228*, 1185–1196. [[CrossRef](#)]
32. Abido, M.A.; Bakhshwain, J.M. Optimal VAR dispatch using a multiobjective evolutionary algorithm. *Int. J. Electr. Power* **2005**, *27*, 13–20. [[CrossRef](#)]
33. Wu, J.N.; Yan, S.Z.; Xie, L.Y. Reliability analysis method of a solar array by using fault tree analysis and fuzzy reasoning Petri net. *Acta Astronaut.* **2011**, *69*, 960–968. [[CrossRef](#)]
34. Gao, M.M.; Zhou, M.C.; Huang, X.G.; Wu, Z.M. Fuzzy reasoning Petri nets. *IEEE Trans. Syst. Man Cybern. A Syst. Hum.* **2003**, *3*, 314–324.
35. Liu, H.-C.; You, J.-X.; Li, Z.W.; Tian, G. Fuzzy Petri nets for knowledge representation and reasoning: A literature review. *Eng. Appl. Artif. Intell.* **2017**, *60*, 45–56. [[CrossRef](#)]
36. Hai, S.X.; Gong, Z.T.; Li, H.X. Generalized differentiability for n-dimensional fuzzy-number-valued functions and fuzzy optimization. *Inf. Sci.* **2016**, *374*, 151–163. [[CrossRef](#)]
37. Nieto, P.J.G.; García-Gonzalo, E.; Lasheras, F.S.; Juez, F.J.D. Hybrid PSO–SVM-based method for forecasting of the remaining useful life for aircraft engines and evaluation of its reliability. *Reliab. Eng. Syst. Saf.* **2015**, *138*, 219–231. [[CrossRef](#)]
38. Yi, P.; Wei, K.; Kong, X.; Zhu, Z. Cumulative PSO-Kriging model for slope reliability analysis. *Probab. Eng. Mech.* **2015**, *39*, 39–45. [[CrossRef](#)]
39. Li, Z.; Zhu, Z.; Song, Y.; Wei, Z. A multi-objective particle swarm optimizer with distance ranking and its applications to air compressor design optimization. *Trans. Meas. Control* **2012**, *34*, 526–556. [[CrossRef](#)]
40. Liu, H.; Miao, E.M.; Wei, X.Y.; Zhuang, X.D. Robust modeling method for thermal error of CNC machine tools based on ridge regression algorithm. *Int. J. Mach. Tools Manuf.* **2017**, *113*, 35–48. [[CrossRef](#)]



© 2017 by the authors. Licensee MDPI, Basel, Switzerland. This article is an open access article distributed under the terms and conditions of the Creative Commons Attribution (CC BY) license (<http://creativecommons.org/licenses/by/4.0/>).